
GENHOP: AN IMAGE GENERATION METHOD BASED ON SUCCESSIVE SUBSPACE LEARNING *

Xuejing Lei
Media Communications Lab
University of Southern California
Los Angeles, CA, USA
xuejing@usc.edu

Wei Wang
Media Communications Lab
University of Southern California
Los Angeles, CA, USA
wang890@usc.edu

C.-C. Jay Kuo
Media Communications Lab
University of Southern California
Los Angeles, CA, USA
jckuo@usc.edu

ABSTRACT

Being different from deep-learning-based (DL-based) image generation methods, a new image generative model built upon successive subspace learning principle is proposed and named GenHop (an acronym of Generative PixelHop) in this work. GenHop consists of three modules: 1) high-to-low dimension reduction, 2) seed image generation, and 3) low-to-high dimension expansion. In the first module, it builds a sequence of high-to-low dimensional subspaces through a sequence of whitening processes, each of which contains samples of joint-spatial-spectral representation. In the second module, it generates samples in the lowest dimensional subspace. In the third module, it finds a proper high-dimensional sample for a seed image by adding details back via locally linear embedding (LLE) and a sequence of coloring processes. Experiments show that GenHop can generate visually pleasant images whose FID scores are comparable or even better than those of DL-based generative models for MNIST, Fashion-MNIST and CelebA datasets.

Keywords Image Generative Modeling · Image Generation · Successive Subspace Learning

1 Introduction

Unconditional image generation has received increasing attention recently due to impressive results offered by deep-learning (DL) based methods such as generative adversarial networks (GANs), variational auto-encoders (VAEs), and flow-based methods. Yet, DL-based methods are blackbox tools. The end-to-end optimization of networks is a non-convex optimization problem, which is mathematically intractable. Being motivated by the design of other generative models that allow mathematical interpretation, a new image generative model is proposed in this work. Our method is developed based on the successive subspace learning (SSL) principle [1, 2, 3, 4] and built upon the foundation of the PixelHop++ architecture [5]. Thus, it is called Generative PixelHop (or GenHop in short). Its high-level idea is sketched below.

Since high-dimensional input images have complicated statistical correlations among pixel values, it is difficult to generate images directly in the pixel domain. To address this problem, GenHop contains three modules: 1) high-to-low dimension reduction, 2) seed image generation, and 3) low-to-high dimension expansion. In the first module, it

**Cite as:* Xuejing Lei, Wei Wang and C.-C. Jay Kuo, “GENHOP: an image generation method based on successive subspace learning,” IEEE International Symposium on Circuits & Systems (ISCAS), Austin, Texas, USA May 28-June 1, 2022.

builds a sequence of high-to-low dimensional subspaces through a sequence of whitening processes called the channel-wise Saab transform, where high frequency components are discarded to lower the dimension. In the second module, the sample distribution in the lowest dimensional subspace can be analyzed and generated by white Gaussian noise, which is called seed image generation. In the third module, GenHop attempts to find the corresponding source image of a seed image through dimension expansion and a coloring mechanism. For dimension expansion, discarded high frequency components are recovered via locally linear embedding (LLE). The coloring process is the inverse of the whitening process, which is achieved by the inverse Saab transform. Experiments are conducted on MNIST, Fashion-MNIST and CelebA three datasets to demonstrate that GenHop can generate visually pleasant images whose FID scores are comparable with (or even better than) those of DL-based generative models.

2 Review of Related Work

DL-based Generative Models. An image generative model learns the distribution of image samples from a certain domain and then generates new images that follow the learned distribution. Generally speaking, the design of image generative models involves analysis and generation two pipelines. The former analyzes properties of training image samples while the latter generates new images after the training is completed. Only the generation unit is used for image generation in inference. So far, the best performing image generative models are all DL-based. We may categorize DL-based generative methods into two categories: adversarial and non-adversarial models. For the adversarial category, generative adversarial networks (GANs) [6] demand that distributions of training and generated images are indistinguishable. This can be achieved by training a generator/discriminator pair through end-to-end optimization of a certain cost function. GANs exhibit good generalization capability and yield visually impressive images. For the non-adversarial category, examples include Variational Auto-Encoders (VAEs) [7], flow-based methods [8, 9] and GLANN [10]. VAEs learn an approximation of the density function with an encoder/decoder structure. Flow-based methods transform the Gaussian distribution into a complex distribution by applying a sequence of invertible transformation functions. GLANN [10] maps images to a feature space obtained by GLO [11] and maps the feature space to the noise space via IMLE [12]. It achieves the state-of-the-art performance among non-adversarial methods.

SSL. Traditional spectral analysis such as the Fourier transform and the principle component analysis (PCA) attempts to capture the global structure but sacrifices local detail (e.g., object boundaries) of images. In contrast, local detail can be well described in the spatial domain, yet the pure spatial representation cannot capture the global information well. To overcome these shortcomings, Kuo *et al.* [1, 2, 3, 4] proposed two affine transforms that determine a sequence of joint spatial-spectral representations of different spatial/spectral trade-offs to characterize the global structure and local detail of images at the same time. They are the Saak transform [3] and the Saab transform [4]. As a variant of the Saab transform, the channel-wise (c/w) Saab transform [5] exploits weak correlations among spectral channels and applies the Saab transform to each channel individually to reduce the model size without sacrificing the performance. The mathematical theory is named successive-subspace-learning (SSL). PixelHop [13] and PixelHop++ [5] are two architectures developed to implement SSL. PixelHop consists of multi-stage Saab transforms in cascade. PixelHop++ is an improved version of PixelHop by replacing the Saab transform with the c/w Saab transform. SSL has been successfully applied to many application domains. Examples include [14, 15, 16, 17, 18, 19, 20, 21, 22, 23, 24, 25]. It is worthwhile to mention that SSL-based texture synthesis was studied in [26, 27]. Here, we examine SSL-based image generation that goes beyond texture and demands a few extensions such as improved fine detail generation, quality enhancement via local detail generation, etc.

3 Proposed GenHop Method

An overview of the proposed GenHop method is shown in Fig. 1, which contains three modules as elaborated below.

3.1 Module 1: High-to-Low Dimension Reduction

A sequence of high-to-low dimensional subspaces is constructed from the source image space S_0 through PixelHop++ [5] as shown in the figure. Each PixelHop++ unit behaves like a whitening operation. It decouples a local neighborhood (i.e., a block) into DC and AC parts and conducts the principal component analysis (PCA) on the AC part. This is named the Saab transform. The reason to remove the DC first is that the ensemble mean of AC part can be well approximated by zero so that the PCA can be applied without the need to estimate the ensemble mean. The PCA is essentially a whitening process. It removes the correlation between AC components among pixels in the same block.

To give an example, for an input gray-scale image of size 28x28, we apply the Saab transform to 2x2 non-overlapping blocks, which offers one DC and three AC channels per block, in the first PixelHop unit. The output is a joint-spatial-spectral representation of dimension 14x14x4, which forms subspace S_1 . We can partition spectral channels

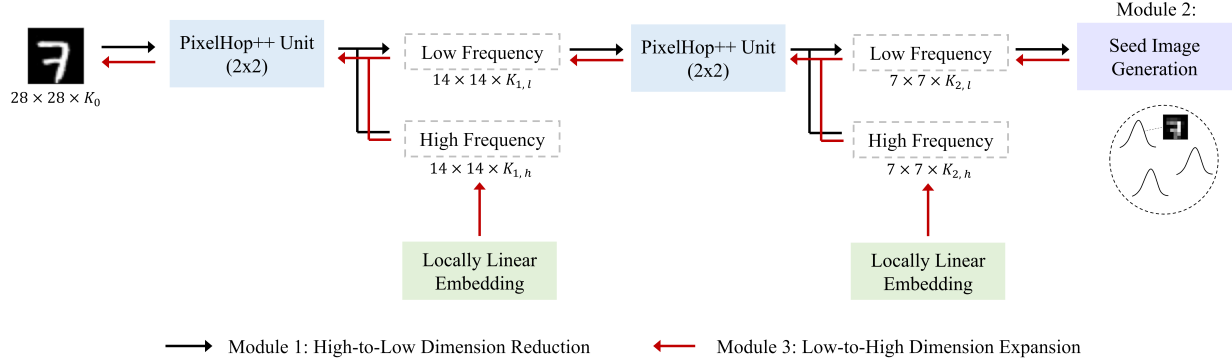


Figure 1: An overview of the GenHop method. Four subspaces S_1, S_2, S_3 and S_4 are constructed from source image space S_0 with two PixelHop++ units. GenHop contains three modules: 1) High-to-Low Dimension Reduction, 2) Seed Image Generation and 3) Low-to-High Dimension Expansion.

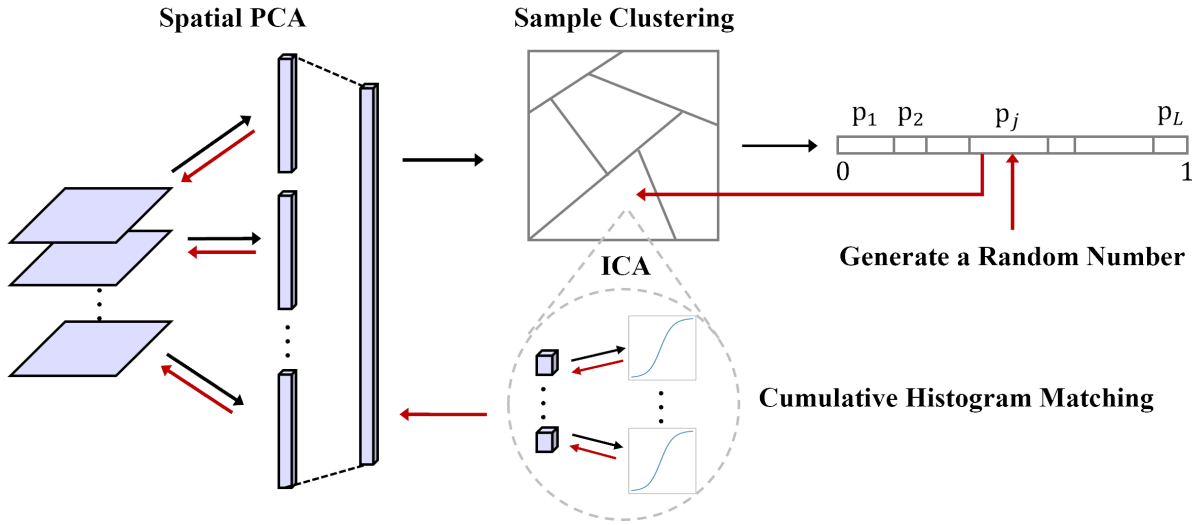


Figure 2: Illustration of seed image generation in the lowest-dimensional subspace.

into low- and high-frequency channels whose numbers are denoted by $K_{1,l}$ and $K_{1,h}$, respectively. Low-frequency channels have larger energy representing the main structure of an image while high-frequency channels has lower energy representing image details. Only low-frequency channels proceed to the next stage. In other words, high-frequency channels are discarded to lower the dimension and will be estimated via LLE as discussed in Sec. 3.3. High-frequency channels with sufficiently small energy will not be estimated, for example, on MNIST dataset. This lead to the sum of $K_{1,l}$ and $K_{1,h}$ being less than 4. The cascade of several PixelHop++ units yields several subspaces. For images of small spatial resolutions, we adopt two PixelHop++ units as shown in Fig. 1 to ensure a proper spatial resolution in S_4 , which has the lowest joint spatial-spectral dimension, to capture the global structure of an image.

3.2 Module 2: Seed Image Generation

In the training phase, we conduct the following four steps to learn the sample distributions in the lowest dimension furthermore, as illustrated in Fig. 2.

1. **Spatial PCA.** There exist correlations between spatial pixels S_4 . They can be removed by applying PCA to the spatial dimension of each channel, called spatial PCA. Components with eigenvalues less than a threshold, γ , are discarded. The reduced subspace and its dimension are denoted by \hat{S}_4 and \hat{D}_4 , respectively. After a sequence of whitening operations, elements of these vector samples are uncorrelated. However, they may still be dependent. Furthermore, they are not Gaussian distributed.

2. **Sample Clustering.** Given training samples in \tilde{S}_4 , we perform k-means clustering on them to generate multiple clusters so that the sample distribution of each cluster can be simplified. This is especially essential for multi-modal sample distributions.
3. **Independent Component Analysis (ICA).** We perform ICA in each cluster to ensure elements of vector samples are independent.
4. **Cumulative Histogram Matching.** We would like to match the cumulative histogram of each independent component in a cluster with that of a Gaussian random variable of zero mean and unit variance [26, 27].

In the generation phase, we conduct the following steps, which are the inverse of the operations as described above.

1. **Cluster Selection.** The probability of selecting a cluster is defined by the ratio of the number of samples in that cluster and the total number of samples in \tilde{S}_4 . We randomly select a cluster based on its probability.
2. **Sample Generation.** We generate a random variable using the Gaussian density of zero mean and unit variance and map it to the corresponding value of the sample distribution in the cluster via inverse cumulative histogram matching.
3. **Inverse ICA.** It rebuilds dependency among elements of random vectors.
4. **Inverse Spatial PCA.** It rebuilds spatial correlations among pixels of each channel.

3.3 Module 3: Low-to-High Dimension Expansion

Recovering Discarded Details via LLE. The generated sample in S_4 contains only low-frequency (LF) components since high-frequency (HF) components are discarded to simplify the seed generation procedure. HF responses should be generated along the reverse direction to enhance details. We adopt LLE [28] to achieve this task. LLE is a commonly used technique to build the correspondence between low- and high-resolution images in image super-resolution [29] or restoration [30]. Here, LLE is used to adjust generated LF samples to ensure two things. First, generated LF samples are located on the manifold of training LF samples. Second, we determine the correspondence between samples of LF components only and samples of both LF and HF components. LLE is implemented in small regions of spatial resolutions 2×2 or 3×3 .

Neighborhood Coloring via inverse Saab Transform. Finally, we build the correlations among spatial pixels via the inverse Saab transform, which can be interpreted as a coloring process. The Saab transform parameters are determined by PCA of AC components of a local neighborhood. The parameters of the inverse transform can be derived accordingly.

4 Experiments

Experimental Setup. We conduct experiments on three datasets: MNIST, Fashion-MNIST and CelebA. They are often used for unconditional image generation. MNIST and Fashion-MNIST contain gray-scale images (i.e. $K_0 = 1$) while CelebA contains RGB color images. To remove the correlation between R, G, B three color channels, we perform pixel-wise PCA to decouple them, yielding three uncorrelated channels denoted by P, Q and R. We discard the R channel that has the smallest eigenvalue to reduce the dimension. To recover the RGB channels, we apply LLE conditioned on generated P and Q channels. As a result, $K_0 = 2$ for CelebA. Hyper-parameters ($K_{1,l}, K_{1,h}, K_{2,l}, K_{2,h}$) are set to (2, 1, 4, 3), (2, 2, 4, 4) and (3, 1, 4, 4) for MNIST, Fashion-MNIST and CelebA, respectively. They are chosen to ensure the gradual dimension transition between two successive subspaces. The eigenvalue threshold, γ , is set to 0.01, 0.01 and 0.03 for MNIST, Fashion-MNIST and CelebA, respectively. The number of nearest neighbors in LLE is adaptively chosen and upper bounded by 3. For CelebA, since the number of training samples of LLE from S_1 to S_0 is high, we perform LLE at one location at a time.

Performance Comparison. We compare the performance of GenHop with several representative DL-based generative models in Table 1. The performance metric is the Fréchet Inception Distance (FID) score. It is commonly used since both diversity and fidelity of generated images are considered. By following the procedure described in [36], we extract the embedding of 10K generated and 10K real images from the test set obtained by the Inception network and fit them into two multivariate Gaussians, respectively. The difference between the two Gaussians are measured by the Fréchet distance with their mean vectors and covariance matrices. A smaller FID score means better performance. The FID scores of representative GAN-based models (listed in the first section of Table 1) are collected from [36] while those of non-adversarial models (the second section) are taken from [10]. We see from the table that Genhop has the

Table 1: Comparison of FID scores of the GenHop model and representative adversarial and non-adversarial models. The lowest FID scores are shown in bold while the second lowest FID scores are underlined.

	MNIST	Fashion	CelebA
MM GAN [6]	9.8	29.6	65.6
NS GAN [6]	6.8	26.5	55.0
LSGAN [31]	7.8	30.7	53.9
WGAN [32]	<u>6.7</u>	21.5	41.3
WGAN-GP [33]	20.3	24.5	30.0
DRAGAN [34]	7.6	27.7	42.3
BEGAN [35]	13.1	22.9	38.9
VAE [7]	23.8	58.7	85.7
GLO [11]	49.6	57.7	52.4
GLANN [10]	8.6	13.0	46.3
Ours (GenHop)	5.1	<u>18.1</u>	<u>40.3</u>

best FID score for MNIST and the second best for Fashion-MNIST and CelebA. Our method outperforms almost all other DL-based benchmarking methods.

Generated Exemplary Images. Some exemplary images generated by GenHop are shown in Fig. 3, Fig. 4 and Fig. 5 for visual quality inspection. For MNIST, the structure of digits is well captured by GenHop with sufficient diversity. For Fashion-MNIST, GenHop generates diverse examples for different classes. Fine details such as texture on shoes and printing on T-shirts can be synthesized naturally. For CelebA, the great majority of samples generated by GenHop are semantically meaningful and realistic. The color of some generated objects is not natural. This failure is attributed to the lack of global information since LLE is only performed in a small region of an image.

5 Conclusion and Future Work

A non-DL-based image generation method, called GenHop, was proposed in this work. To summarize, GenHop conducted the following tasks: 1) removing correlations among pixels in a local neighborhood via the Saab transform, 2) discarding high frequency components for dimension reduction, 3) generating seed images in the lowest dimensional space using white Gaussian noise, 4) adding back discarded high frequency components for dimension expansion based on LLE and 5) recovering correlations of pixels via the inverse Saab transform. Tasks #1 and #2 can be done in multiple stages. Similarly, tasks #4 and #5 can also be executed in multiple stages. GenHop achieved state-of-the-art performance for MNIST, Fashion-MNIST and CelebA the datasets in FID scores. As future extension, it is desired to use GenHop to generate images of higher resolution and more complicated content. It is also interesting to apply GenHop to the context of transfer learning (e.g., transfer between horses and zebras) and image inpainting.

Acknowledgment

This research was supported by a gift grant from Mediatek. Computation for the work was supported by the University of Southern California’s Center for High Performance Computing (hpc.usc.edu).

References

- [1] C-C Jay Kuo. Understanding convolutional neural networks with a mathematical model. *Journal of Visual Communication and Image Representation*, 41:406–413, 2016.
- [2] C-C Jay Kuo. The cnn as a guided multilayer recos transform [lecture notes]. *IEEE signal processing magazine*, 34(3):81–89, 2017.
- [3] C-C Jay Kuo and Yueru Chen. On data-driven saak transform. *Journal of Visual Communication and Image Representation*, 50:237–246, 2018.
- [4] C-C Jay Kuo, Min Zhang, Siyang Li, Jiali Duan, and Yueru Chen. Interpretable convolutional neural networks via feedforward design. *Journal of Visual Communication and Image Representation*, 2019.
- [5] Yueru Chen, Mozhdeh Rouhsedaghat, Suyu You, Raghuvveer Rao, and C-C Jay Kuo. Pixelhop++: A small successive-subspace-learning-based (ssl-based) model for image classification. *arXiv preprint arXiv:2002.03141*, 2020.
- [6] Ian Goodfellow, Jean Pouget-Abadie, Mehdi Mirza, Bing Xu, David Warde-Farley, Sherjil Ozair, Aaron Courville, and Yoshua Bengio. Generative adversarial nets. In *Advances in neural information processing systems*, pages 2672–2680, 2014.
- [7] Diederik P. Kingma and Max Welling. Auto-Encoding Variational Bayes. In *2nd International Conference on Learning Representations, ICLR 2014, Banff, AB, Canada, April 14-16, 2014, Conference Track Proceedings*, 2014.
- [8] Laurent Dinh, David Krueger, and Yoshua Bengio. Nice: Non-linear independent components estimation. *arXiv preprint arXiv:1410.8516*, 2014.
- [9] Laurent Dinh, Jascha Sohl-Dickstein, and Samy Bengio. Density estimation using real nvp. *arXiv preprint arXiv:1605.08803*, 2016.
- [10] Yedid Hoshen, Ke Li, and Jitendra Malik. Non-adversarial image synthesis with generative latent nearest neighbors. In *Proceedings of the IEEE Conference on Computer Vision and Pattern Recognition*, pages 5811–5819, 2019.
- [11] Piotr Bojanowski, Armand Joulin, David Lopez-Pas, and Arthur Szlam. Optimizing the latent space of generative networks. In *International Conference on Machine Learning*, pages 600–609, 2018.
- [12] Ke Li and Jitendra Malik. Implicit maximum likelihood estimation. *arXiv preprint arXiv:1809.09087*, 2018.
- [13] Yueru Chen and C-C Jay Kuo. Pixelhop: A successive subspace learning (ssl) method for object recognition. *Journal of Visual Communication and Image Representation*, page 102749, 2020.
- [14] Hong-Shuo Chen, Mozhdeh Rouhsedaghat, Hamza Ghani, Shuowen Hu, Suyu You, and C-C Jay Kuo. Defakehop: A light-weight high-performance deepfake detector. In *2021 IEEE International Conference on Multimedia and Expo (ICME)*, pages 1–6. IEEE, 2021.
- [15] Kaitai Zhang, Bin Wang, Wei Wang, Fahad Sohrab, Moncef Gabbouj, and C-C Jay Kuo. Anomalyhop: an ssl-based image anomaly localization method. In *2021 International Conference on Visual Communications and Image Processing (VCIP)*, pages 1–5. IEEE, 2021.
- [16] Pranav Kadam, Min Zhang, Shan Liu, and C-C Jay Kuo. R-pointhop: A green, accurate and unsupervised point cloud registration method. *arXiv preprint arXiv:2103.08129*, 2021.
- [17] Xiaofeng Liu, Fangxu Xing, Chao Yang, C-C Jay Kuo, Suma Babu, Georges El Fakhri, Thomas Jenkins, and Jonghye Woo. Voxelhop: Successive subspace learning for als disease classification using structural mri. *arXiv preprint arXiv:2101.05131*, 2021.
- [18] Min Zhang, Yifan Wang, Pranav Kadam, Shan Liu, and C-C Jay Kuo. Pointhop++: A lightweight learning model on point sets for 3d classification. In *2020 IEEE International Conference on Image Processing (ICIP)*, pages 3319–3323. IEEE, 2020.
- [19] Min Zhang, Haoxuan You, Pranav Kadam, Shan Liu, and C-C Jay Kuo. Pointhop: An explainable machine learning method for point cloud classification. *IEEE Transactions on Multimedia*, 2020.
- [20] Min Zhang, Pranav Kadam, Shan Liu, and C-C Jay Kuo. Unsupervised feedforward feature (uff) learning for point cloud classification and segmentation. In *2020 IEEE International Conference on Visual Communications and Image Processing (VCIP)*, pages 144–147. IEEE, 2020.
- [21] Pranav Kadam, Min Zhang, Shan Liu, and C-C Jay Kuo. Unsupervised point cloud registration via salient points analysis (spa). In *2020 IEEE International Conference on Visual Communications and Image Processing (VCIP)*, pages 5–8. IEEE, 2020.

- [22] Abinaya Manimaran, Thiyagarajan Ramanathan, Suyu You, and C-C Jay Kuo. Visualization, discriminability and applications of interpretable saak features. *Journal of Visual Communication and Image Representation*, 66:102699, 2020.
- [23] Tzu-Wei Tseng, Kai-Jiun Yang, C-C Jay Kuo, and Shang-Ho Tsai. An interpretable compression and classification system: Theory and applications. *IEEE Access*, 8:143962–143974, 2020.
- [24] Mozhddeh Rouhsedaghat, Yifan Wang, Xiou Ge, Shuowen Hu, Suyu You, and C-C Jay Kuo. Facehop: A lightweight low-resolution face gender classification method. *arXiv preprint arXiv:2007.09510*, 2020.
- [25] Mozhddeh Rouhsedaghat, Masoud Monajatipoor, Zohreh Azizi, and C-C Jay Kuo. Successive subspace learning: An overview. *arXiv preprint arXiv:2103.00121*, 2021.
- [26] Xuejing Lei, Ganning Zhao, and C.-C. Jay Kuo. Nites: A non-parametric interpretable texture synthesis method. In *2020 Asia-Pacific Signal and Information Processing Association Annual Summit and Conference (APSIPA ASC)*, pages 1698–1706, 2020.
- [27] Xuejing Lei, Ganning Zhao, Kaitai Zhang, and C-C Jay Kuo. Tghop: An explainable, efficient and lightweight method for texture generation. *arXiv preprint arXiv:2107.04020*, 2021.
- [28] Sam T Roweis and Lawrence K Saul. Nonlinear dimensionality reduction by locally linear embedding. *science*, 290(5500):2323–2326, 2000.
- [29] Hong Chang, Dit-Yan Yeung, and Yimin Xiong. Super-resolution through neighbor embedding. In *Proceedings of the 2004 IEEE Computer Society Conference on Computer Vision and Pattern Recognition, 2004. CVPR 2004.*, volume 1, pages I–I. IEEE, 2004.
- [30] Chun-Ting Huang, Zhengning Wang, and C.-C. Jay Kuo. Visible-light and near-infrared face recognition at a distance. *Journal of Visual Communication and Image Representation*, 41:140–153, 2016.
- [31] Xudong Mao, Qing Li, Haoran Xie, Raymond YK Lau, Zhen Wang, and Stephen Paul Smolley. Least squares generative adversarial networks. In *Proceedings of the IEEE international conference on computer vision*, pages 2794–2802, 2017.
- [32] Martin Arjovsky, Soumith Chintala, and Léon Bottou. Wasserstein generative adversarial networks. In *International Conference on Machine Learning*, pages 214–223, 2017.
- [33] Ishaan Gulrajani, Faruk Ahmed, Martín Arjovsky, Vincent Dumoulin, and Aaron C Courville. Improved training of wasserstein gans. In *NIPS*, 2017.
- [34] Naveen Kodali, Jacob Abernethy, James Hays, and Zsolt Kira. On convergence and stability of gans. *arXiv preprint arXiv:1705.07215*, 2017.
- [35] David Berthelot, Thomas Schumm, and Luke Metz. Began: Boundary equilibrium generative adversarial networks. *arXiv preprint arXiv:1703.10717*, 2017.
- [36] Mario Lucic, Karol Kurach, Marcin Michalski, Sylvain Gelly, and Olivier Bousquet. Are gans created equal? a large-scale study. In *Advances in neural information processing systems*, pages 700–709, 2018.

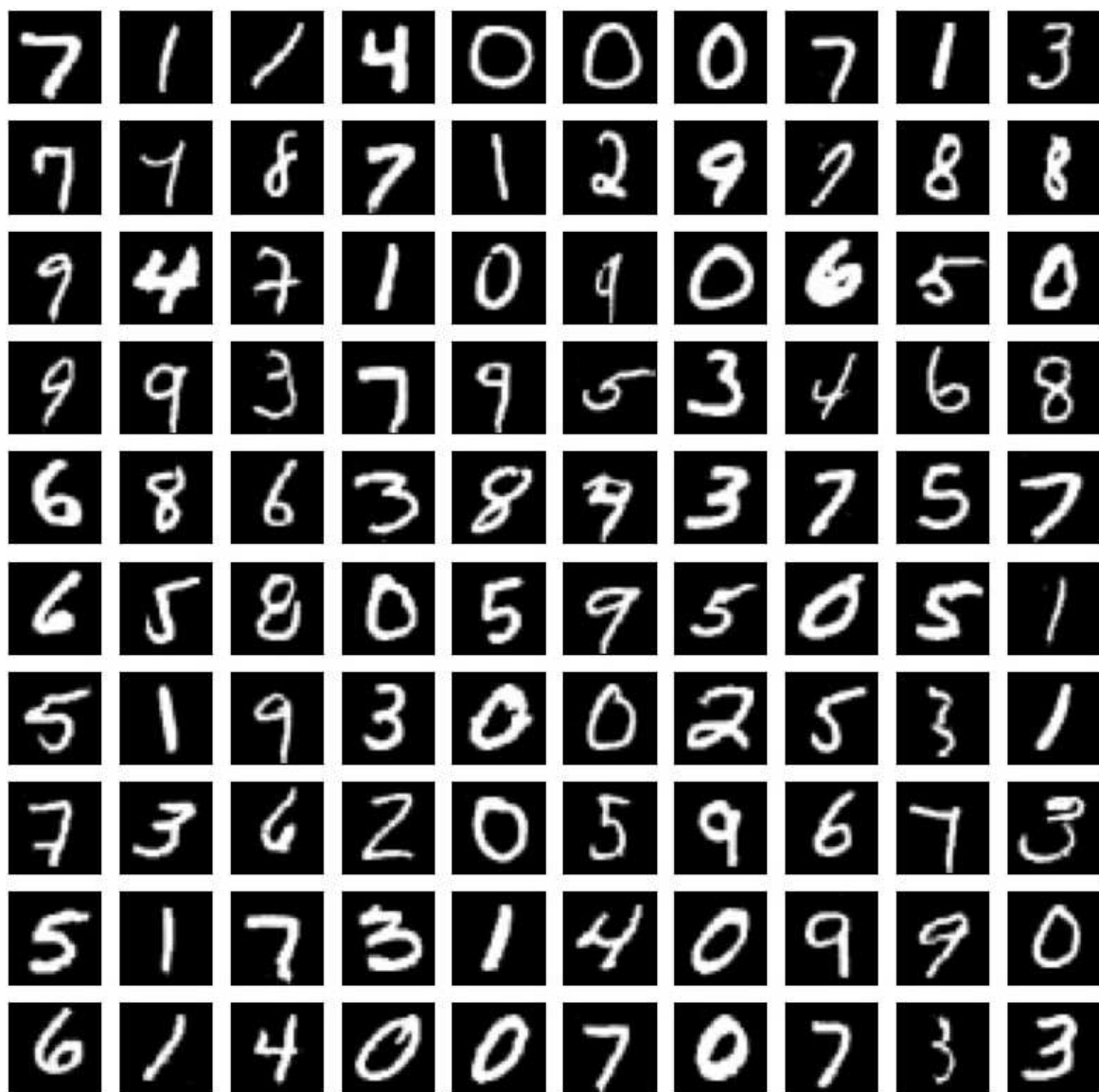


Figure 3: Exemplary images generated by GenHop with training samples from the MNIST dataset.



Figure 4: Exemplary images generated by GenHop with training samples from the Fashion-MNIST dataset.



Figure 5: Exemplary images generated by GenHop with training samples from the CelebA dataset.